Published in final edited form as:
Physiol Genomics. ; 15(3): 177–190. doi:10.1152/physiolgenomics.00062.2003.

Array analysis of gene expression in connexin-43 null astrocytes

Dumitru A. Iacobas, **Marcia Urban-Maldonado**, **Sanda Iacobas**, **Eliana Scemes**, and **David C. Spray**
Department of Neuroscience, Albert Einstein College of Medicine, New York 10461

Abstract

Connexin-43 (Cx43) is the most abundant gap junction protein in brain, where it is found primarily between astrocytes. Although the morphology of astrocytes from Cx43-null (knockout, KO) mice is similar to that of wild-type (WT) astrocytes, KO astrocytes exhibit reduced growth rate in culture. To evaluate the impact of deletion of Cx43 on other genes, including those encoding cell cycle proteins, we used DNA arrays to determine expression patterns in cultured astrocytes from sibling Cx43-null and WT mice. RNA samples extracted from astrocytes cultured from WT and Cx43-null neonatal mice were dye labeled and individually cohybridized with a reference of labeled cDNAs pooled from a variety of tissues on 8 gene arrays containing 8,975 mouse DNA sequences. Normal variability in expression of each gene was evaluated and incorporated into "expression scores" to statistically compare expression levels between WT and KO samples. In Cx43-null astrocytes, 4.1% of the 4,998 adequately quantifiable spots were found to have significantly ($P < 0.05$) decreased hybridization compared with controls, and 9.4% of the spots showed significantly higher hybridization. The significantly different spots corresponded to RNAs encoding 252 known proteins, many not previously linked to gap junctions, including transcription factors, channels and transporters, cell growth and death signals, enzymes and cell adhesion molecules. These data indicate a surprisingly high degree of impact of deletion of Cx43 on other astrocyte genes, implying that gap junction gene expression alters numerous processes in addition to intercellular communication.

Keywords

glia; gap junction; knockout; DNA array; intercellular communication

CONNEXIN-43 (Cx43, also termed gap junction alpha-1, GJA1) was the second gap junction protein whose cDNA was cloned and sequenced (3), which was accomplished by low-stringency screening of heart cDNA libraries with Cx32 cDNA. It is the most widespread gap junction protein in mammals, where it occurs in almost every tissue (3,5,6). Cx43 is the primary component of intercellular gap junction channels in ventricular myocytes of the heart (50) and in astrocytes (9,43), the most abundant type of glial cells in the brain. Cx43 also occurs between neural progenitors in early development (14,45,46) and in leptomeningeal, ependymal, and vascular cells (10,11).

Cx43-null mice die at birth due to a developmental cardiac abnormality, where hyperplasia blocks blood flow exiting from the right ventricular outflow tract to the lungs (44); other

Address for reprint requests and other correspondence: D. A. Iacobas, Albert Einstein College of Medicine, Dept. of Neuroscience, Kennedy Center, Rm. 915C, 1300 Morris Park Ave, Bronx, NY 10461 (E-mail: diacobas@aecom.yu.edu)..

Article published online before print. See web site for date of publication (http://physiolgenomics.physiology.org).

GRANTS

This work was supported in part by National Institutes of Health Grants NS-41023 (to E. Scemes), NS-42807, NS-41282, and MH-65495 (to D. C. Spray).

congenital abnormalities include coronary artery patterning defects (28). Brains of Cx43-null mice are grossly normal (8,39), although it has been reported that migration of cardiac neural crest cells is altered compared with wild-type (WT) littermates (57) and that neocortical neuronal migration is delayed in Cx43-null mice (15).

Because of its requirement for proper cardiac function, alterations in Cx43 expression and/or function are associated with a large variety of cardiac arrhythmic disorders (27,40), and mice deficient in Cx43 gene expression exhibit abnormal cardiac conduction and are prone to reentry (35). Alterations in Cx43 expression have also been detected in transcriptomic studies of Huntington's and Alzheimer's diseases (33,54), in autoimmune inflammation (6,32), and in astrocytomas (17). Mutations in other gap junction genes result in peripheral neuropathy, deafness, and cataracts (55). Although the association of Cx43 missense mutations with the complex disorder heterovisceral atriotaxia has been controversial (4,48), more recent studies have suggested that Cx43 mutations are responsible for hypoplastic left heart syndrome (7), rare cases of non-syndromic deafness (31), and oculodentodigital dysplasia (38); Cx43 mutations have also been reported in metastatic colon tumors (12).

One phenotypic difference between astrocytes cultured from Cx43-null mice compared with wild types is a profound reduction in their growth rate (8,36). Previous studies on Cx43-transfected glioma cells had demonstrated that some highly expressing stable clones exhibited decreased proliferation, which has subsequently been attributed to the increased expression in Cx43 transfectants of genes encoding secreted growth suppressive molecules (see Ref. 37 for overview of these studies). Moreover, recent studies have suggested that the growth suppression in Cx43-transfected cells may be independent of the formation of intercellular gap junction channels (34,42), although in some studies intercellular communication is required or enhances the expression of growth suppression molecules (16,59).

Cx43 expression has also recently been linked to programmed cell death. Cx43 overexpression in human glioblastoma cells was shown to increase sensitivity of the cells to a variety of chemotherapeutic agents and under conditions of low serum, which was correlated with decreased expression of the anti-apoptotic bcl-2 protein (18,20). However, transfection with Cx43 has also been reported to protect the cells from cell injury, either through a mechanism involving nonjunctional hemichannels or not requiring functional channels at all (29,41).

A growing number of studies suggest that connexin proteins may play functional roles supplemental to their unique mediation of direct intercellular communication. In addition to effects on growth rate and apoptosis considered above, purinergic receptor expression is altered in Cx43-null astrocytes from brain and spinal cord (47,52), and cell adhesion appears to depend on connexin expression but not on coupling strength (30). Although some of these effects may be mediated by connexin-protein interactions, which normally assemble a macromolecular complex (13,49), it is also possible that connexin expression may affect cell phenotype through alterations in the expression of other genes. Indeed, differential mRNA display analysis has identified a number of gene alterations in Cx43-transfected glioma cells (35), and use of cytokine arrays has identified changes in certain proteins following Cx43 transfection (19). To test this hypothesis for a large number of genes, we have compared gene expression in sibling WT and Cx43-null mouse astrocytes using cDNA microarrays. Our findings indicate a surprisingly high degree of alteration in gene expression in astrocytes from Cx43-null mice, with many of the known genes on the arrays being statistically up- or downregulated. Moreover, a number of these genes encode proteins involved in cell cycle control and apoptosis, consistent with phenotypic differences in growth rate of Cx43-deficient astrocytes and with previous linkage of Cx43 expression to cellular sensitivity to apoptotic stimuli.

MATERIALS AND METHODS

The study was conducted according to standards developed by the Microarray Gene Expression Data Society (MGED), and data complying with the "minimum information about microarray experiments" (MIAME) have been deposited in the National Center for Biotechnology Information (NCBI) Gene Expression Omnibus (GEO) database, and can be accessed at **http://www.ncbi.nlm.nih.gov/geo/** (platform GPL369, samples GSM8889 to GSM8896).

RNA sources

Heterozygous $Cx43^{+/-}$ mice (44), obtained from Jackson Laboratories (Bar Harbor, ME), in the C57BL/6j background, were interbred in our AALAC-accredited animal facilities to obtain WT and Cx43-null progeny. At birth, brains of individual mice were dissected free of meninges in cold PBS, minced, and dissociated in trypsin (0.1%). Cells were then resuspended in DMEM with 10% fetal bovine serum and 1% penicillin-streptomycin and seeded in tissue culture flasks. One week later, flasks were shaken overnight to remove less adherent cells. After trypsinization (0.05% trypsin), cells were plated in 100-mm culture dishes for 1 wk (WT) or 2 wk (Cx43 null), at which time they were confluent (about 225 cells/mm^2). Medium was replaced every 2–3 days during culture. Genotype of each animal was determined by PCR of tail DNA as described (8). At 2 days after the last feeding, RNA was isolated using the TRIzol method (see **http://www.aecom.yu.edu/home/molgen/funcgenomic.html**); parallel dishes were used for cell density determination and staining with glial fibrillary protein antibodies (Sigma polyclonal anti-GFAP, 1:500). Purity of cultures was 91–92% GFAP-positive cells; neurons and oligodendrocytes were absent as judged by morphology of GFAP-negative cells. No difference in percentage of GFAP-positive cells was detected between WT and Cx43-null astrocyte cultures (see Ref. 8). Mouse reference RNA (hereafter denoted by *R*) was prepared at one time in sufficient quantity for the entire projected experiment from selected amounts of total RNA extracted from 10 adult male and female mouse tissues (aorta, brain, heart, kidney, liver, lung, ovary/testicles, spleen, and stomach), in a combination that provided a very high diversity of moderately well-expressed genes.

Construction and hybridization of labeled cDNAs

A total of 40 μg RNA from *R* and extracted from each of four confluent 100-mm-diameter dishes of cultured astrocytes, each isolated from distinct neonatal WT or Cx43-null mice, was reverse transcribed into cDNA using fluorescent dUTPs [Cy3-dUTP, excited at 532 nm (green), and Cy5-dUTP, excited at 635 nm (red)]. The labeled cDNAs were hybridized overnight at 50°C on 10 aminosilane-coated Corning glass slides, spotted with 8,975 selected mouse DNA sequences in 16 pen-domains (provided by the Albert Einstein College of Medicine Microarray Facility; array code 15M) in the combinations indicated in Table 1. After hybridization, the slides were washed at room temperature, using solutions containing 0.1% sodium dodecyl sulfate (SDS) and 1% SSC (3 M NaCl + 0.3 M sodium citrate) to remove the nonhybridized cDNAs. The experimental design and the usage of an invariant reference eliminate the bias introduced by the direct incorporation of fluorescent dyes during the reverse transcription reaction (24), since the extracts which are compared have the same label (here green) and the reference unit (here red labeled) is constant.

Scanning, data acquisition, and normalization

The microarrays were scanned with an Axon GenePix 4000A scanner using the same PMT settings (750 V at 635 nm, 670 V at 532 nm) and maintained throughout the entire experiment, and data were acquired through GenePix Pro 4.0 software (**http://www.axon.com**). We considered only spots *s* (of each array γ) for which the means of the foreground signals (*F*) were significantly ($P < 0.001$) higher than those of the background signals (*B*) in both channels. Thus the cut-off conditions (denoted as "635cut-off" and "532cut-off") of valid spots were

$$\frac{F635mean(\gamma;s)-B635mean(\gamma;s)}{\sqrt{\frac{[F635SD(\gamma;s)]^2}{Fpixels(\gamma;s)}+\frac{[B635SD(\gamma;s)]^2}{Bpixels(\gamma;s)}}}>3,\quad \frac{F532mean(\gamma;s)-B532mean(\gamma;s)}{\sqrt{\frac{[F532SD(\gamma;s)]^2}{Fpixels(\gamma;s)}+\frac{[B532SD(\gamma;s)]^2}{Bpixels(\gamma;s)}}}>3 \quad (1)$$

where symbols are those from the gpr file provided by GenePix Pro 4.0 software, and "3" is the critical value of the standard score establishing that the means of the foreground and background pixel intensities are statistically different ($P < 0.001$).

The raw data were first corrected according a previously published procedure (25) to minimize various noise sources (26), then normalized to make them comparable (4). In addition to the composite within-array normalization (58) intended to balance the net fluorescence readings of the two channels within each array, a similar composite between-array normalization was used to balance the net reference readings from all arrays.

Gene expression indicators

The expression ratio of the gene identified by the spot *s* in the Cx43-null cortical astrocytes (*K*) compared with the WT (*W*) was computed as

$$x(s;W\rightarrow K)\equiv\frac{\left\langle\frac{\psi532(\gamma;s)}{\psi635(\gamma;s)}\right\rangle\Big|^{\text{all } RrKg \text{ chips}}}{\left\langle\frac{\psi532(\gamma;s)}{\psi635(\gamma;s)}\right\rangle\Big|^{\text{all } RrWg \text{ chips}}} \quad (2)$$

where γ indicates the array hybridized with cDNAs from *R* and *W* or *R* and *K*, and ψ532(γ;*s*)/ψ635(γ;*s*) designates the arithmetic mean of the corrected fluorescence net ratio of the spot *s* in the array γ hybridized with the red-labeled reference and green-labeled extract of Cx43-null astrocytes, *RrKg*, or with the red-labeled reference and the green-labeled extract of WT astrocytes, *RrWg*.

The *P* value of the up- or downregulation can be determined through the one-tailed *t*-test for different (unknown) population variances

$$P(s)-val=ttest(\{\psi532(\gamma;s)\}\Big|^{\text{all } RrKg \text{ chips}},\{\psi532(\gamma;s)\}\Big|^{\text{all } RrWg \text{ chips}},1,3) \quad (3)$$

where {ψ532(γ;*s*)} is the set of corrected green readings of the spot *s* in all arrays hybridized with *RrKg* or *RrWg*.

The observed regulation is significant if the expression score (τ)

$$\tau(s;W\rightarrow K;P)=\frac{\left\langle\frac{\psi532(\gamma;s)}{\psi635(\gamma;s)}\right\rangle\Big|^{\text{all } RrKg \text{ chips}}-\left\langle\frac{\psi532(\gamma;s)}{\psi635(\gamma;s)}\right\rangle\Big|^{\text{all } RrWg \text{ chips}}}{\sqrt{\frac{[n_K(s)-1]Var\left(\frac{\psi532(\gamma;s)}{\psi635(\gamma;s)}\right)\Big|^{\text{all } RrKg \text{ chips}}+[n_W(s)-1]Var\left(\frac{\psi532(\gamma;s)}{\psi635(\gamma;s)}\right)\Big|^{\text{all } RrKg \text{ chips}}}{n_K(s)+n_W(s)-2}\times\left(\frac{1}{n_K(s)}+\frac{1}{n_W(s)}\right)}} \quad (4)$$

falls in the critical region

$$\left(-\infty, t\left(n_K(s)+n_W(s)-2;\frac{P}{2}\right)\right) \cup \left(\left|t\left(n_K(s)+n_W(s)-2;\frac{P}{2}\right)\right|, \infty\right) \quad (5)$$

where $t(n_K(s) + n_W(s) - 2;P/2)$ is the negative P-significant Student critical value, and $n_A(s)$ is the number of arrays hybridized as *RrKg* (or *RrWg*) in which the spot s was adequately quantified.

For all significantly regulated genes, values are presented in tables for the expression ratio value (x), as well as $\log_2 x$, where the binary logarithm was chosen to symmetrize the values for up- and downregulation with the same factor [e.g., $x = 8 \rightarrow \log_2 8 = 3$ and $x = 1/8 = 0.125 \rightarrow \log_2(1/8) = -3$]. Note that the 16-bit detection system limits the logarithm of the expression ratio to the interval (−16, +16). Positive τ values indicate upregulation, while negative τ values indicate downregulation, with the risk P.

Transcription patholog

Using the expression scores, we built the pre-Hilbert space of the transcriptomic profiles having as many dimensions as distinct genes that were adequately quantified; every point of this space is a possible transcriptome (here of cortical astrocytes), and every curve is a possible transcriptomic evolution (22). For each significantly regulated gene, we determined the ratio between the absolute score, $|\tau(s;W \rightarrow K;P)|$, and the positive limit of the critical region, $|t(n_K(s) + n_W(s) - 2;P/2)|$, and then we summed the differences between each ratio and the unit. The percent ratio between the obtained sum and the number of adequately quantified genes was termed the transcription patholog, which quantifies the overall significant alteration of the expression of adequately quantified genes (23).

Variability (REV) and stability (GES) of gene expression

We defined the P-significant relative estimated variability (REV) of the gene identified by the spot s in the specimen A (= W, K) as the midrange chi-squared (χ^2) interval estimate of the standard deviation compared with the average corrected signal.

Because of the asymmetry of the REV distribution (expressed by the skewedness value, see Results), this indicator cannot be used to categorize the genes according to their expression variability. Therefore, we introduced the gene expression stability (GES) as the percentile that locates the gene's REV in the inversely ordered sequence of REV values of all adequately quantified genes.

These measurements of variability and stability of transcription are not redundant; REV provides an estimation of transcriptional control, whereas GES integrates the studied genes in the general picture of GES within a particular specimen, eliminating the variability introduced by preparations of different types of samples.

Coordinated transcriptomics

The analysis of expression coordination makes it possible to group the genes that regulate each other in various experimental conditions and may ultimately allow identification of "command gene" within every group of interest.

The Pearson correlation coefficient (21)

$$\rho(s1,s2;A)=\frac{CoVar(\log_2[\psi532(\gamma;s1)],\log_2[\psi532(\gamma;s2)])\Big|^{\text{all RrAg chips}}}{\sqrt{Var(\log_2[\psi532(\gamma;s1)])\Big|^{\text{all RrAg chips}}\times Var(\log_2[\psi532(\gamma;s2)])\Big|^{\text{all RrAg chips}}}} \quad (6)$$

was used to determine the degree of expression coordination of the genes probed by the spotted sequences s_1 and s_2 within the specimen A (= W, K). The correlation coefficient yields values from −1 to +1. Positive correlation indicates that the expressions of both genes increase and decrease simultaneously in a series of extracts, and negative correlation indicates inverse expression tendencies, whereas a value close to zero indicates that the variations of expression levels of the two genes are independent. The statistical significance of the correlation coefficient is strongly dependent on the number of replications. In our case of four replications, the 5% cutoffs are $|\rho| > 0.9$ for coordination and $|\rho| < 0.05$ for independence, whereas the 10% cutoffs are $|\rho| > 0.8$ for coordination and $|\rho| < 0.1$ for independence. Moderate correlations ($0.1 \le |\rho| \ge 0.8$) were eliminated from the analysis as not statistically significant.

A major problem in the coordinated transcriptomic analysis is the manipulation of hundreds of millions of correlation coefficients at a time. To limit the calculations to manageable data sets, it is currently necessary to preselect the classes of genes to be considered and then to construct the coordination topology by aggregating the small groups. We hypothesized that transcription coordination among the genes related in a functional pathway might be conserved among genotypes. Therefore, we studied the transcription coordination of the genes related to the cell cycle-shape-differentiation and cell death pathways (see Results) within the WT astrocytes that were found to be significantly up- or downregulated in the Cx43-null astrocytes.

We defined the coordination power (COP) of a gene to show the percentage contribution of that gene to the total correlations within a group of selected genes for each genotype. One goal of our studies has been to introduce an objective criterion by which to choose the most prominent (or “command”) gene for every group and report the coordination of all other genes to it. Therefore, we identified the most prominent gene as the one combining the highest correlation (COP) power against the others within its group with the maximum expression stability (GES); the term given for the product of COP and GES is gene prominence (GP).

RESULTS

The α-step (Table 1) revealed that hybridization of 6,909 out of the 8,975 spots were adequately quantifiable and therefore useful for further analysis. For affected genes, accession numbers were reblasted using **http://www.informatics.jax.org** and **http://www.ncbi.nlm.nih.gov** to update the gene description from that given on the platform file for the 15M mouse microarray (**http://biotech.aecom.yu.edu:7778/web/aecomarray.html**).

Expression variability for individual spots and genotype-specific differences

To determine the significance of changes in observed gene expression ratio, the normal variability for each quantifiable spot among individual WT and Cx43-null astrocytes was first determined (β- and γ-steps in Table 1). The histograms of REV are shown in Fig. 1*A* for 3,032 spots that were quantifiable in all four arrays from WT astrocytes and in Fig. 1*B* for the 3,593 spots that were quantifiable in each of four arrays from Cx43-null astrocytes. A comparison of these histograms indicates that the mean and standard deviation REV values were lower for WT than for Cx43-null astrocytes. Moreover, the histogram of REV values for the WT astrocytes displayed a slightly sharper peak than for Cx43-null astrocytes (as quantified by skewedness and kurtosis values presented in Fig. 1, *A* and *B*). Both distributions were slightly positively oriented (as quantified by skewedness values).

The slight apparent differences in overall distribution of REV values raised the question of whether the REV values of individual genes were similar in WT and Cx43-null astrocytes. To address this issue, the REV value for each spot from WT astrocytes was plotted against the REV value for the same spot from Cx43-null astrocytes (Fig. 1*C*). This analysis revealed a surprising degree of independence of spot variability in WT compared with Cx43-null astrocytes. This independence was most apparent when comparing REV values of spots that were highly variable (REV > 100) in one or the other genotype. For example, in both WT and Cx43 knockout (KO) astrocytes, virtually all genes with REV > 100 in one genotype showed REV < 100 in the other genotype. Regression analysis revealed that the two sets of REV values are independent at $P < 0.05$, consistent with the apparent independence for spots with the highest REV values.

The most and least variable spots for which the genes were identifiable in WT astrocytes are listed in Tables 2 and 3, where REV values are given for each gene in Cx43-null astrocytes as well. In addition, values are presented for GES, a parameter that indicates the normalized rank order of stability in each genotype (see Materials and Methods).

As expected from the independence of REV values illustrated in Fig. 1*C*, the degree of expression stability of certain genes was dramatically different in the WT and Cx43-null astrocytes. For example, some genes converted from being highly controlled to highly fluctuant (e.g., immunoglobulin κ-chain joining region and procollagen-lysine 2-oxoglutarate 5-dioxygenase 1; *notes A* and *B* in Table 2), and some genes changed from highly fluctuant to highly stable (e.g., UDP-glucose dehydrogenase and ribosomal protein L44; *notes A* and *B* in Table 3). However, a small number of genes preserved their character of being highly stably or highly unstably transcribed in the astrocytes following deletion of the Cx43 gene. For instance, ganglioside-induced differentiation-associated protein 2 (*note 1* in Table 2), zinc finger protein 275 (*note 2*, Table 2), proteasome subunit-α type 4 (*note 3*, Table 3), ubiquitin conjugating enzyme 7 interacting protein (*note 4*, Table 2), torsin family 3 member 1A (*note 5*, Table 2), and adaptor-related protein complex AP1 μ-subunit 1 (*note 6*, Table 2) were very stable in astrocytes of both genotypes, whereas aquaporin 1 (*note 1* in Table 3), biglycan (*notes 2a*, *2b*, and *2c*, Table 3), secreted modular calcium binding protein 2 (*note 3*, Table 3), and low-density lipoprotein receptor (*note 4*, Table 3) were highly unstable in both groups. It should be noted that one of these genes (biglycan, bolded and *notes 2a*, *2b*, and *2c* in Table 3) was represented by three DNA spots; in all three cases and in both genotypes, this gene exhibited a high degree of variability. The similar REV values for each of these spots in WT and in Cx43-null astrocytes provided further validation of the reproducibility of the measurements.

As indicated below, we have analyzed the coordination among expression of genes related to programmed cell death. Interestingly, disruption of Cx43 increased the average transcription variability among these genes from 37.6% to 58.9%, suggesting a relaxation of the transcription control of these genes in the Cx43-null astrocytes.

Differences in expression levels of individual genes in WT and Cx43-null astrocytes

Hybridization of the cDNA microarrays with labeled RNA extracts led to quantifiable signals for at least 3 of 4 samples from both genotypes for 4,998 of the spots. Of these, 206 (4.1%) of the spotted sequences showed significantly ($P < 0.05$) less hybridization in the Cx43-null astrocytes, and 468 (9.4%) showed significantly higher hybridization. When corrected for redundancy and expressed sequence tag (ESTs) removed, the number of significantly altered genes in Cx43 KO astrocytes was reduced to 252. Of the 252 identified genes that were altered in Cx43-null astrocytes, 35% (88 genes) were downregulated and 65% (164) were upregulated (Fig. 2*A*).

A complete list of the 252 identified genes whose expression was significantly different in Cx43-null and WT astrocytes is given in the Supplemental Table A (available at the *Physiological Genomics* web site),[1] along with the expression ratio (x), its binary logarithm ($\log_2 x$) and P values. To begin to assign the functionalpathways to which these gene products belong, we have classified them according to biological functions within the cell (2). The 10 categories in which we have grouped the altered genes are as follows: junction-adhesion-extracellular matrix (JAE, which includes antigens, globulins, integrins, claudins, cadherins, connexins, desmosomal components, laminin, proteoglycans, etc.); cytoskeletal (CY, which includes intermediary filaments, microtubules, centrioles, actin, and their associated proteins); transport into the cell (T1, which includes channels, transporters, and ionotropic receptors); transport within the cell (T2, which includes proteins of vesicles, cellular motors, endosomes, lysosomes, nuclear transport, protein folding, etc.); cell signaling (CS, which includes G protein-coupled receptors, protein kinases, SH2 and SH3 domain proteins, calcium binding proteins, etc.); cell cycle-shape-differentiation (CSD, which includes growth factors, apoptosis-related genes, cytokines, etc.); transcription (TR, which includes DNA binding proteins, DNA repair, RNA, transcription factors, oncogenes, etc.); energy and metabolism (EnMet, which includes oxidants, peroxisomes, respiratory chain, glycolysis and glycogenesis, enzymes, etc.); organelle genetics (OG, which consists of mitochondrial genes); and genes encoding proteins for which function is presently unknown (UNKf).

A pie chart of the classes of all statistically altered genes ($P < 0.05$) in Cx43-null astrocytes is presented in Fig. 2*B*. Of the 252 altered genes, 7% had unknown function (UNKf), 29% were related to TR, 19% to En-Met, 9% to JAE, 9% to CS, 9% to T2, and 8% to CSD. The remaining 9% of the altered genes were about equally distributed among the other three categories (Fig. 2*B*).

Pie charts depicting the distributions of up- and downregulated genes in Cx43-null compared with WT astrocytes are presented in Fig. 2, *C* and *D*. Comparison of the proportions of genes that were upregulated and downregulated in each functional category reveals overall similarity as well as some interesting differences. For example, a higher percentage of TR genes (32 vs. 25%) and almost three times the percentage of T2 genes (12 vs. 4.5%) were upregulated than down-regulated in the Cx43-null astrocytes, whereas a higher percentage of JAE genes (11 vs. 7.3%) and a greater percentage of EnMet genes (24 vs. 17%) were downregulated in the Cx43-null astrocytes. With regard to transcripts encoding proteins involved in cell cycle and cell growth control, we detected about the same percentage upregulated (7.3%) as downregulated (9.1%). These regulated genes included upregulation of fibroblast growth factor 1 (FGF-1), fractalkine, BMP1, growth arrest and DNA-damage-inducible 45β, and Bcl2-like; the most highly downregulated CSD genes included platelet factor 4, septin 3, and LIM only 2. Moreover, transcription factors acting on the cell cycle were affected; notably, axin (a component of the Wnt signaling pathway, which together with Smt3 is involved in β-catenin degradation) and p53 (a transcription factor that induces cell cycle arrest) were upregulated in Cx43-null astrocytes.

Overall change in transcriptome of Cx43-null astrocytes

The global alteration of the transcriptome was evaluated by calculating the value of the transcription patholog (see Materials and Methods). When all genes were considered, the calculated patholog was 2.4%. This value is twice that calculated for the patholog in Cx43-null brains (D. A. Iacobas, unpublished results), which presumably is attributable to the more

[1]The Supplementary Material for this article (Supplemental Table A, complete list of the 252 identified genes whose expression was significantly different in Cx43-null and WT astrocytes) is available online at **http://physiolgenomics.physiology.org/cgi/content/full/00062.2003/DC1**.

homogeneous population of Cx43 expressing cells in cultured astrocytes than in the whole brain.

Coordinated transcriptomics of cell cycle/shape/differentiation genes

We and others (8,34) have previously reported that the growth rate of astrocytes cultured from Cx43-null mice is dramatically slower than that of WT astrocytes. To determine whether genes involved in growth and differentiation were coordinately regulated in WT astrocytes and to examine genotype-related changes in this regulation, we have calculated correlation coefficients for each pair of the CSD genes found to be significantly altered for all arrays.

Of the 20 significantly regulated genes classified as encoding proteins with CSD functions, 16 were adequately quantifiable on all four arrays from both genotypes and therefore suitable for the coordination analysis. Correlation coefficients for each pair of selected genes are presented in the form of a coordination diagram in Fig. 3, where lines between the boxed genes indicate significant correlation in WT astrocytes and numbers represent the correlation coefficients between the WT expression ratios (highlighted values indicate antagonistic coordination). Colors indicate whether the gene was found to be significantly upregulated (red) or downregulated (green) in Cx43-null astrocytes. This analysis revealed 17 significant correlations, including 3 triangular associations, where the 3 correlation coefficients were consistent with the coordination of each of the others (Fig. 3*A*). In 4 cases out of 17 (all within the bottom cluster in Fig. 3*B*), regulations in Cx43-null astrocytes were opposite to that predicted by the correlation coefficients. Nevertheless, 77% of the significantly coordinated pairs of genes in WT astrocytes accurately predicted the significant regulation of these genes in the Cx43-null astrocytes.

Based on the correlation coefficients and the GES, we have calculated the COP and the GP of the CSD genes, which are listed in Table 4. Interestingly, the coordination powers (COP values) are confined in a relatively narrow interval (4.91% to 6.81%), with cyclin-dependent kinase inhibitor 2C (Cdkn2c) showing the least coordination with the other CSD genes, and growth arrest and DNA-damage-inducible 45β (Gadd45b) having the highest COP score. By contrast, the expression stability (GES) of these genes spans a large range of percentiles (12.63 to 88.26), with N-myc downstream regulated 3 (Ndr3) the least stable and Gadd45b having the highest stability.

As a consequence of its highest coordination power (COP = 6.81%) and highest stability (GES = 88.26), Gadd45b was identified as the most prominent gene of the CSD class (GP = 11.81%), followed closely by Cdk2 (GP = 11.62%), Cdk9 (GP = 10.04%), and similar to mitotic control protein dis3 (Mcpd3) (GP= 10.66%). As predicted by the antagonistic coordination with Gadd45b and Cdk9, Cdk2 was downregulated in Cx43-null astrocytes while the other two were upregulated. Mcpd3 is remarkable in that its downregulation in Cx43-null astrocytes is opposite to the antagonistic coordinations with Cx3cl1 and Bcl2-like. In addition to these significantly correlated expression patterns, we identified the following pairs of CSD genes whose expression was significantly independent ($P < 0.05$) in WT astrocytes: myeloid-associated differentiation marker (Myadm) and both N-myc downstream regulated 3 (Ndr3) and myeloid associated differentiation marker (Myadm) with cyclin-dependent kinase inhibitor 2C (Cdkn2c), septin 3 (Sep3) and LIM only 2 (Lmo2), and platelet factor 4 (Pf4) with fractalkine (Cx3cl1).

Coordinated transcriptomics of apoptotic genes

As an additional strategy to search for coordinated gene expression within functional pathways and to investigate the relationship between Cx43 expression and apoptosis, we extended our coordinated transcriptomic analysis to genes related to programmed cell death. For this

analysis, we selected all adequately expressed genes related to programmed cell death within WT astrocytes, using as a guide the pathway map compiled by Apotech (**http://www.apotech.ch**), with gene synonyms obtained from Online Mendelian Inheritance in Man (OMIM; NCBI).

Our analysis in WT astrocytes of 24 programmed cell death-related genes whose expression was quantifiable on all arrays revealed that for most of these genes there was highly significant synergistic or antagonistic expression with at least one other gene in this group. In addition, gene expression was significantly independent for some pairs. The significant positive and negative relationships are summarized in the coordination diagram shown in Fig. 4, where the solid lines indicate correlations that are highly significant ($P < 0.05$; numbers represent correlation coefficients calculated in WT astrocytes). As can be seen from the solid lines in Fig. 4, the majority of highly significant correlation coefficients were for positive regulation [20 were significantly synergistic (red lines), compared with 8 antagonistic relations (blue lines)].

The prominence sequence of the analyzed apoptotic genes (where numbers indicate GP values) is: Apaf1 (7.49) > Tnfrsf10b (6.61) > Map2k1ip1 (6.57) > Ube2i (6.47) > Cdk2 (6.45) > Casp2 (6.23) < Prkacb (6.17) > Hspb2 (5.67) > Birclc (4.40) > Prnp (4.24) > Nfkb2 (4.06) > Cdk9 (3.96) > Map3k1 (3.83) > Bircla (3.70) > Map4k5 (3.41) > Map3k3 (3.14) > Rasa3 (2.92) > Prkaca (2.72) > Casp1 (1.84) > Cd4 (1.46) > Bak1 (1.18) > Tnfaip2 (1.1) > Akt2 (0.9). Therefore, for these apoptotic pathway genes, our analysis indicates that the most prominent genes are apoptotic protease activating factor 1 (Apaf1) and tumor necrosis factor receptor super-family member 10b (Tnfrsf10b or Trail2), whereas the least prominent is thyoma viral protooncogene 2 (Akt2).

Expression of 8 of the 24 quantifiable apoptotic genes was significantly altered in Cx43-null astrocytes (Fig. 4, red boxes indicate upregulation, green boxes down-regulation). In all cases but one, significantly regulated genes were highly correlated with expression of at least one other gene in this pathway. Whereas some of these up- and downregulations in Cx43-null astrocytes were as expected from the correlation linkages determined in WT astrocytes (e.g., the Nfkb2 cluster), others were not, suggesting that correlations among the genes might be altered in Cx43-null astrocytes. Calculations of correlation coefficients between each pair of the 24 quantifiable apoptotic genes revealed global changes, with 10.6% of the correlations being significantly increased and 16.2% being significantly reduced.

We further found that the proportion of the coexpressed genes was higher in Cx43 KO astrocytes (13.4% compared with 7.1%), indicating an enhanced coupling among apoptotic genes in the Cx43-deficient cells. It is also interesting to note that the proportion of antagonistically coexpressed pairs increased from 2.7% in WT to 8.9% in KO, suggesting an enhanced reciprocal negative control of these genes; the proportion of significant synergistic coordination was slightly reduced (from 6.1% in WT to 4.7% in Cx43-null astrocytes). The most stably and the most unstably expressed genes in the WT astrocytes were apoptotic protease activating factor 1 ($GES_{Apaf1} = 98.9\%$) and thyoma viral protooncogene 2 ($GES_{Akt2} = 12.5\%$).

Correlation patterns in the Cx43-null astrocytes were similar to those seen in WT astrocytes. Functional stability (FS), defined as the weighted average of GES values by the COP values, was calculated for WT and Cx43-null astrocytes. Functional stability of the moderately stable apoptotic pathway (FS = 56.8%) was found to be slightly diminished by the disruption of Cx43 (FS = 46.5%).

DISCUSSION

We have quantitatively analyzed 9k DNA arrays in which labeled cDNA from four WT and four Cx43-null sibling mice were hybridized against a pooled reference obtained from a variety of mouse tissues. To statistically compare expression levels in each gene between genotypes, we have determined the variability in expression ratio (REV) for each spot in each genotype and then incorporated the variability in calculations of expression ratio (x) to obtain gene expression scores (τ). Because these scores incorporate variability, they permit statistical comparison of gene expression without using arbitrary cutoff thresholds in ratio values.

One finding from these calculations was that the variability of individual gene expression ratios spanned a wide range in both WT and Cx43-null astrocytes. Although low REV values indicate tight transcriptional control and high REV values indicate loose control, we have not yet attempted to address the implied issue of whether high or low variability might reflect genes whose functions segregate with cellular housekeeping or with cellular specialization. However, the REV values for individual spots in one genotype were statistically independent of REV values for the same spots in the other genotype. This is an interesting finding, suggesting that "compensation" or "adaptation" for the loss of one gene may change the degree of transcriptional control for a wide range of individual genes with unrelated functions.

When expression scores were analyzed, a large number of spots were found to differ significantly between genotypes, and the significantly altered spots surprisingly corresponded to a large number of identified genes with functions apparently unrelated to intercellular communication. As noted in the Introduction, this finding is consistent with a number of recent reports describing effects of connexin expression on cell growth, apoptosis, and purinergic receptor expression (16,34,42,59,31,41,47,52,30), not all of which require formation of functional gap junction channels. Numerous mechanisms may be responsible for such profound changes in gene expression, including those related to developmental events that may depend on intercellular communication or functionally compensate for its loss. Because Cx43 is a gap junction protein that is expressed at earliest times during embryogenesis (53), loss of Cx43 might be predicted to exert particularly global effects on subsequent development, where changes in expression might reflect functional adaptation. Studies to evaluate this possibility are underway using astrocytes treated acutely with anti-sense oligonucleotides to reduce Cx43 expression (52). Alternatively, or in addition, there may be direct feedback, so that Cx43 or its binding partners may act directly or indirectly to transactivate or inactivate the other genes. Such a mechanism has been identified involving β-catenin interaction with Cx43, whereby β-catenin exerts a transcriptional control that is modulated by the interaction between β-catenin and Cx43 at the junctional membrane (1). Moreover, "connexin response elements" have been proposed to modulate gene expression in osteocytes (51).

To evaluate whether Cx43 deletion selectively affected genes with specific functions, we have categorized the identified genes according to 10 functions of encoded proteins. This simple classification allowed us to select 16 regulated genes involved in cell cycle regulation for detailed analysis of coordinated expression. Our analysis of the coordination among the genes and alterations in the Cx43-null astrocytes may be interpreted to provide a mechanistic basis for the slowed growth rates of Cx43-null than WT astrocytes in culture (8,36). For example, upregulation of Gadd45b (which activates p38 and JNK pathways), Ndr3 (which may decrease cyclin D1), FGF1 (which promotes exit from cell cycle), and requiem (which is required for apoptosis) may all favor decreased cell proliferation. Moreover, downregulation of Cdk2 (which is necessary for G_2-M phase transition), Lmo2 (which is an important factor in early development), Myadm (a myeloid differentiation factor), Septin 3 (which is a key factor in late steps of cytokinesis), and the relative of Dis3 (Mcpd3, which is another required mitotic signal) may act directly to slow cell growth. Indirect effects through transcription factors may also

participate, as indicated by the upregulation of axin and p53 (which directly and indirectly slow cell growth).

The central hypothesis of our coordinated expression analysis is that genes encoding proteins with synergistic or antagonistic functions might be coordinately expressed, in contrast to genes encoding proteins with independent functions. Consistent with this hypothesis, the coordinated transcriptomic analysis predicted most of the up- and downregulated CSD genes in the Cx43-null astrocytes, with the exception of the interactions of Set3 and Mcpd3 with Cx3cl1 and Bcl2-like. This finding that the correlations of variations in the expression of a gene of interest and other genes among different animals largely predicts changes in the knockout further indicates that the correlations are robust. This type of analysis of other pathways may provide a methodological key to promote general understanding of synergistic, antagonistic, and independent intracellular signaling.

Both increased and decreased resistance to cell injury have previously been associated with Cx43 expression (18,20,29,41). Our analysis of the coordinated expression of genes associated with programmed cell death involved calculations of correlation coefficients among all possible pairs of the 24 apoptosis-associated genes adequately expressed on all 8 of the DNA arrays used in these studies. This analysis revealed that both pro-apoptotic and anti-apoptotic genes were up- and downregulated in Cx43-null astrocytes. Upregulated pro-apoptotic genes include Nfkb2 and Map4k5, both of which selectively activate the JNK pathway, whereas the anti-apoptotic protein Bcl2-like ($BclX_L$, BAX) was also upregulated. The coordination analysis revealed that expressions of other cell death-related genes were strongly correlated, many of which were further correlated with expression of those genes that were altered in Cx43-null astrocytes. For example, Map4k5 was negatively correlated with the Trail-2 receptor (Tnfrsf10b), which was positively correlated with two proteins implicated in neuronal death (Hspb2, Bircla), as well as a protein induced by inflammatory cytokines (Tnfaip2) and an activator of the ERK signaling pathway (Map3k3). These associations suggest that the genes involved in the TNFα and Trail death receptor pathways may be synergistic within the pathways and antagonistic between them. Moreover, these opposite regulations of genes encoding pro- and anti-apoptotic proteins and their complex linkages to the expression of other death pathway proteins may explain in part the reported differences in sensitivity of Cx43 transfectants and Cx43-null cell lines to stimuli that may selectively activate one or another of these pathways. It is important to point out that although these studies have been limited to cultured astrocytes, the findings imply that gene expression changes secondary to Cx43 expression may either enhance or diminish the neuro-protective effects of astrocytes on neurons.

Through the efforts of several laboratories, a number of gap junction genes have now been deleted through homologous recombination, and prominent phenotypic changes have been observed in many but not all of these transgenic mice (see Ref. 56 for recent review). Until now, all phenotypic changes observed in connexin-deficient mice have been attributed to the absence of intercellular channels in tissues where they are normally expressed. A caveat of such studies, and of the present analysis as well, is the lack of control for the neomycin phosphotransferase gene inserted to disrupt the coding region in the Cx43-null mice. Nevertheless, the findings reported in this paper indicate that astrocytes from Cx43-null mice show up- and downregulation of many other genes with diverse functions and thus suggest that gap junction genes regulate multiple cellular processes. Functional changes observed in either deletion or overexpression studies may thus not only reveal the function of gap junction channels in the organ of interest, but may also reflect changes in expression of other genes induced by the manipulation.

Acknowledgements

We are grateful to Frances Andrade for editorial/secretarial assistance.

References

1. Ai Z, Fischer A, Spray DC, Brown AMC, Fishman GI. Wnt-1 regulation of Cx43 in cardiac myocytes. J Clin Invest 2000;105:161–171. [PubMed: 10642594]
2. Alberts, B.; Bray, D.; Lewis, J.; Raff, M.; Roberts, K.; Watson, JD. Molecular Biology of the Cell. Vol. 3. New York: Garland; 1994.
3. Beyer EC, Paul DL, Goodenough DA. Connexin43: a protein from rat heart homologous to a gap junction protein from liver. J Cell Biol 1987;105:2621–2629. [PubMed: 2826492]
4. Britz-Cunningham SH, Shah MM, Zuppan CW, Fletcher WH. Mutations of the connexin43 gap-junction gene in patients with heart malformations and defects of laterality. N Engl J Med 1995;332:1323–1329. [PubMed: 7715640]
5. Butte A. The use and analysis of microarray data. Nat Rev Drug Discov 2002;1:951–960. [PubMed: 12461517]
6. Carmody RJ, Hilliard B, Maguschak K, Chodosh LA, Chen YH. Genomic scale profiling of autoimmune inflammation in the central nervous system: the nervous system response to inflammation. J Neuroimmunol 2002;133:95–107. [PubMed: 12446012]
7. Dasgupta C, Martinex AM, Zuppan CW, Shah MM, Bailey LL, Fletcher WH. Identification of connexin43 (alpha1) gap junction gene mutations in patients with hypoplastic left heart syndrome by denaturing gradient gel electrophoresis (DGGE). Mutat Res 2001;479:173–186. [PubMed: 11470490]
8. Dermietzel R, Gao Y, Scemes E, Vieira D, Urban M, Kremer M, Bennett MVL, Spray DC. Connexin43 null mice reveal that astrocytes express multiple connexins. Brain Res Rev 2000;32:45–56. [PubMed: 10751656]
9. Dermietzel R, Hertzberg EL, Kessler JA, Spray DC. Gap junctions between cultured astrocytes: immunocytochemical, molecular, and electrophysiological analysis. J Neurosci 1991;11:1421–1432. [PubMed: 1851221]
10. Dermietzel R, Spray DC. Gap junctions in the brain: where, what type, how many and why? Trends Neurosci 1993;16:186–192. [PubMed: 7685944]
11. Dermietzel R, Traub O, Hwang TK, Beyer E, Bennett MV, Spray DC, Willecke K. Differential expression of three gap junction proteins in developing and mature brain tissues. Proc Natl Acad Sci USA 1989;86:10148–10152. [PubMed: 2557621]
12. Dubina MV, Iatckii NA, Popov DE, Vasil'ev SV, Krutovskikh V. Connexin43, but not connexin32, is mutated atadvanced stages of human sporadic colon cancer. Oncogene 2002;21:4992–4996. [PubMed: 12118378]
13. Duffy HS, John GR, Lee SC, Brosnan CF, Spray DC. Reciprocal regulation of the junctional proteins claudin-1 and connexin43 by interleukin-1 primary human fetal astrocytes. J Neurosci 2000;20:RC114. [PubMed: 11090614]
14. Duval N, Gomes D, Calaora V, Calabrese A, Meda P, Bruzzone R. Cell coupling and Cx43 expression in embryonic mouse neural progenitor cells. J Cell Sci 2002;115:3241–3251. [PubMed: 12140256]
15. Fushiki S, Perez Velazquez JL, Zhang L, Bechberger JF, Carlen PL, Naus CC. Changes in neuronal migration in neocortex of connexin43 null mutant mice. J Neuropathol Exp Neurol 2003;62:304–314. [PubMed: 12638734]
16. Goldberg GS, Bechberger JR, Tajima Y, Merritt M, Omori Y, Gawinowicz MA, Marayanan R, Tan Y, Sanai Y, Yamasaki H, Naus CC, Tsuda H, Nicholson BJ. Connexin43 suppresses MFG-E8 while inducing contact growth inhibition of glioma cells. Cancer Res 2000;60:6018–6026. [PubMed: 11085522]
17. Gutmann DH, Hedrick NM, Li J, Nagarajan R, Perry A, Watson MA. Comparative gene expression profile analysis of neurofibromatosis 1-associated, and sporadic pilocytic astrocytomas. Cancer Res 2002;62:2085–2091. [PubMed: 11929829]
18. Huang RP, Hossain MZ, Huang R, Gano J, Fan Y, Boynton AL. Connexin43 (Cx43) enhances chemotherapy-induced apoptosis in human glioblastoma cells. Int J Cancer 2001;92:1301–1338.

19. Huang R, Lin Y, Wang CC, Gano J, Lin B, Shi Q, Boynton A, Burke J, Huang RP. Connexin 43 suppresses human glioblastoma cell growth by down-regulation of monocyte chemotactic protein 1, as discovered using protein array technology. Cancer Res 2002;62:2806–2812. [PubMed: 12019157]
20. Huang R, Liu YG, Lin Y, Fan Y, Boynton A, Yang D, Huang RP. Enhanced apoptosis under low serum conditions in human glioblastoma cells by connexin 43 (Cx43). Mol Carcinog 2001;32:128–138. [PubMed: 11746825]
21. Iacobas, DA. Medical Biostatistics. Vol. 3rd English. Constanta, Romania: Tilia; 1997. p. 180-182.
22. Iacobas DA, Urban M, Iacobas S, Spray DC. The "patholog" of the gene expression profile in evaluating the ecotoxin effects. Adv Ecol Sci 2001;10:733–742.
23. Iacobas DA, Iacobas S, Spray DC. The "patholog" of the genes expression profile, a new tool in defining, evaluating, and classifying the genetic diseases. Rom J Physiol 2000;37:59–67. [PubMed: 12413147]
24. Iacobas DA, Urban M, Massimi A, Spray DC. Improved procedure to mine the spotted cDNA arrays. J Biomol Tech 2002;13:5–19.
25. Iacobas DA, Urban M, Massimi A, Iacobas S, Spray DC. Hits and misses from gene expression ratio measurements in cDNA microarray studies. J Biomol Tech 2002;13:143–157.
26. Ideker T, Thorsson V, Siegel AF, Hood LE. Testing for differentially-expressed genes by maximum-likelihood analysis of microarray data. J Comput Biol 2000;7:805–817. [PubMed: 11382363]
27. Kostin S, Rieger M, Dammer S, Hein S, Richter M, Klovekorn WP, Bauer EP, Schaper J. Gap junction remodeling and altered connexin43 expression in the failing human heart. Mol Cell Biochem 2003;242:135–144. [PubMed: 12619876]
28. Li WE, Waldo K, Linask KL, Chen T, Wessels A, Parmacek MS, Kirby ML, Lo CW. An essential role for connexin43 gap junctions in mouse coronary artery development. Development 2002;129:2031–2042. [PubMed: 11934868]
29. Lin JH, Yang J, Liu S, Takano T, Wang X, Gao Q, Willecke K, Nedergaard M. Connexin mediates gap junction-independent resistance to cellular injury. J Neurosci 2003;23:430–441. [PubMed: 12533603]
30. Lin JH, Takano T, Cotrina ML, Arcuino G, Kang J, Liu S, Gao Q, Jiang L, Li F, Lichtenberg-Frate H, Haubrich S, Willecke K, Goldman SA, Nedergaard M. Connexin 43 enhances the adhesivity and mediates the invasion of malignant glioma cells. J Neurosci 2002;22:4302–4311. [PubMed: 12040035]
31. Liu XZ, Xia XJ, Adams J, Chen ZY, Welch KO, Tekin M, Ouyang XM, Kristiansen A, Pandya A, Balkany T, Arnos KS, Nance WE. Mutations in GJA1 (connexin43) are associated with non-syndromic autosomal recessive deafness. Hum Mol Genet 2001;10:2945–2951. [PubMed: 11741837]
32. Lock C, Hermans G, Pedotti R, Brendolan A, Schadt E, Garren H, Langer-Gould A, Strober S, Cannella B, Allard J, Klonowski P, Austin A, Lad N, Kaminski N, Galli SJ, Oksenberg JR, Raine CS, Heller R, Steinman L. Genemicroarray analysis of multiple sclerosis lesions yields new targets validated in autoimmune encephalomyelitis. Nat Med 2002;8:500–508. [PubMed: 11984595]
33. Loring JF, Wen X, Lee JM, Seilhamer J, Somogyi R. A gene expression profile of Alzheimer's disease. DNA Cell Biol 2001;20:683–695. [PubMed: 11788046]
34. Moorby C, Patel M. Dual functions for connexins: Cx43 regulates growth independently of gap junction formation. Exp Cell Res 2001;271:238–248. [PubMed: 11716536]
35. Morley GE, Vaidya D, Jalife J. Characterization of conductance in the ventricles of normal and heterozygous Cx43 knockout mice using optical imaging. J Cardiovasc Electrophysiol 2000;11:375–377. [PubMed: 10749364]
36. Naus CC, Bechberger JF, Zhang Y, Venance L, Yamasaki H, Juneja SC, Kidder GM, Giaume C. Altered gap junctional communication, intercellular signaling, and growth in cultured astrocytes deficient in connexin43. J Neurosci Res 1997;49:528–540. [PubMed: 9302074]
37. Naus CC, Bond SL, Bechberger JF, Rushlow W. Identification of genes differentially expressed in C6 glioma cells transfected with connexin 43. Brain Res Rev 2000;32:259–266. [PubMed: 10751676]
38. Paznekas WA, Boyadjiev SA, Shapiro RE, Daniels O, Wollnik B, Keegan CE, Innis JW, Dinulos MB, Christian C, Hannibal MC, Jabs EW. Connexin43 (GJA1) mutations cause the pleiotropic phenotype of oculodentodigital dysplasia. Am J Hum Genet 2003;72:408–418. [PubMed: 12457340]

39. Perez-Velazquez JL, Frantseva M, Nauss CC, Bechberger JF, Juneja SC, Velumian A, Carlen PL, Kidder GM, Mills LR. Development of astrocytes and neurons in cultured brain slices from mice lacking connexin43. Brain Res Dev Brain Res 1996;97:293–296.
40. Peters NS, Wit AL. Myocardial architecture and ventricular arrhythmogensis. Circulation 1998;97:1746–1754. [PubMed: 9591770]
41. Plotkin LI, Manolagas C, Bellido T. Transduction of cell survival signals by connexin43 hemichannels. J Biol Chem 2002;277:8648–8657. [PubMed: 11741942]
42. Qin H, Sharo Q, Curtis H, Galipeau J, Belliveau DJ, Want T, Alaoui-Jamali MA, Laird DW. Retroviral delivery of connexin genes to human breast tumor cells inhibits in vivo tumor growth by a mechanism that is independent of significant gap junctional intercellular communication. J Biol Chem 2002;277:29132–29138. [PubMed: 12042301]
43. Rash JE, Yasumura T, Dudek FE, Nagy JI. Cell-specific expression of connexins and evidence of restricted gap junctional coupling between glial cells and between neurons. J Neurosci 2001;21:1983–2000. [PubMed: 11245683]
44. Reaume AG, de Sousa PA, Kulkarni S, Langille BL, Zhu D, Davies TC, Juneja SC, Kidder GM, Rossant J. Cardiac malformation in neonatal mice lacking connexin43. Science 1995;267:1831–1834. [PubMed: 7892609]
45. Rozental R, Morales M, Mehler MF, Urban M, Kremer M, Dermietzel R, Kessler JA, Spray DC. Changes in the properties of gap junctions during neuronal differentiation of hippocampal progenitor cells. J Neurosci 1998;18:1753–1762. [PubMed: 9465000]
46. Rozental R, Srinivas M, Gokhan S, Urban M, Dermitzel R, Kessler JA, Spray DC, Meltzer MF. Temporal expression of neuronal connexins during hippocampal ontogeny. Brain Res Rev 2000;32:57–71. [PubMed: 10751657]
47. Scemes E, Suadicani SO, Spray DC. Intercellular communication in spinal cord astrocytes: fine tuning between gap junctions and P2 nucleotide receptors in calcium wave propagation. J Neurosci 2000;20:1435–1445. [PubMed: 10662834]
48. Splitt MP, Burn J, Goodship J. Connexin43 mutations in sporadic and familial defects of laterality. N Engl J Med 1995;333:941. [PubMed: 7666890]
49. Spray DC, Duffy HS, Scemes E. Gap junctions in glia. Types, roles, and plasticity. Adv Exp Med Biol 1999;468:339–359. [PubMed: 10635041]
50. Spray, DC.; Suadicani, S.; Srinivas, M.; Gutstein, DE.; Fishman, GI. Gap junctions in the cardiovascular system. *Handbook of Physiology. The Cardiovascular System. The Heart*. Bethesda, MD: Am Physiol Soc; 2001. p. 169-212.sect. 2, vol. I, chapt. 4
51. Stains JP, Lecanda F, Screen J, Towler DA, Civitelli R. Gap junctional communication modulates gene transcription by altering recruitment of Sp1 and SP3 to connexin-response elements in osteoblast promoters. J Biol Chem 2003;278:24377–24387. [PubMed: 12700237]
52. Suadicani SO, DePina-Benabou M, Urban-Maldonado M, Spray DC, Scemes E. Acute down-regulation of Cx43 alters P2Y receptor expression levels in mouse spinal cord astrocytes. Glia 2003;42:160–171. [PubMed: 12655600]
53. Valdimarsson G, Kidder GM. Temporal control of gap junction assembly in preimplantation mouse embryos. J Cell Sci 1995;108:1715–1722. [PubMed: 7615688]
54. Vis JC, Nicholson LF, Faull RL, Evans WH, Severs NJ, Green CR. Connexin expression in Huntington's diseased human brain. Cell Bio Int 1998;22:837–847. [PubMed: 10873295]
55. White TW, Paul DL. Genetic diseases and gene knockouts reveal diverse connexin functions. Annu Rev Physiol 1999;61:283–310. [PubMed: 10099690]
56. Willecke K, Eiberger J, Degen J, Eckhardt D, Romualdi A, Guldenagel M, Duetsch U, Sohl G. Structural and functional diversity of connexin genes in the mouse and human genome. Biol Chem 2002;383:725–737. [PubMed: 12108537]
57. Xu X, Li WE, Huang GY, Meyer R, Chen T, Luo Y, Thomas MP, Radice GL, Lo CW. Modulation of mouse neural crest cell motility by N-cadherin and connexin 43 gap junctions. J Cell Biol 2001;154:217–230. [PubMed: 11449002]
58. Yang YH, Dudoit S, Luu P, Lin DM, Peng V, Ngai J, Speed TP. Normalization for cDNA microarray data: a robust composite method addressing single and multiple slide systematic variation. Nucleic Acids Res 2002;30:e15. [PubMed: 11842121]

59. Zhang YW, Morita I, Ikeda M, Ma KW, Murota S. Connexin43 suppresses proliferation of osteosarcoma U2OS cells through post-transcriptional regulation of p27. Oncogene 2001;20:4138–4139. [PubMed: 11464280]

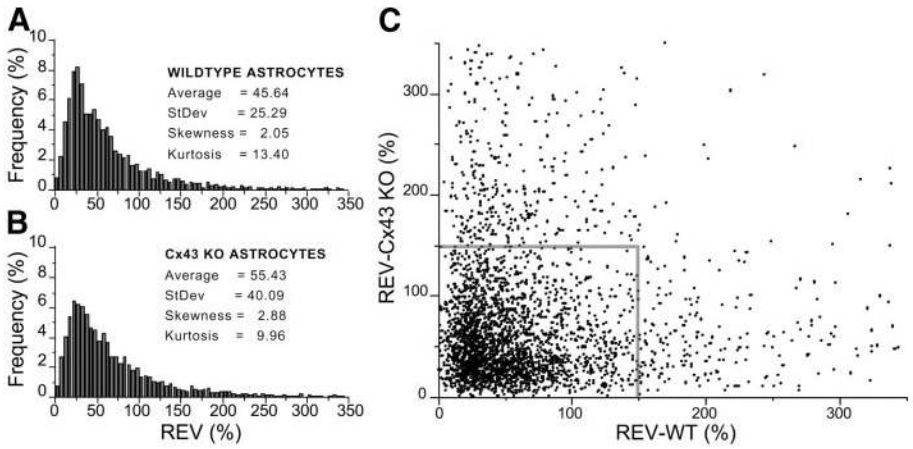

Fig. 1.

Variability in spot hybridization among all four arrays for wild-type (WT) and connexin-43 (Cx43) null astrocytes. *A* and *B*: histogram of relative estimated variability (REV) values for WT and Cx43-null astrocytes. For WT astrocytes, the mean REV value was lower and the distribution more sharply peaked (as reflected in higher kurtosis value). *C*: comparison of the REV values for the individual spots that were quantifiable on all four arrays from both genotypes. Note that spots with REV values >100 in one genotype generally corresponded to much lower REV values in the other genotype. KO, knockout.

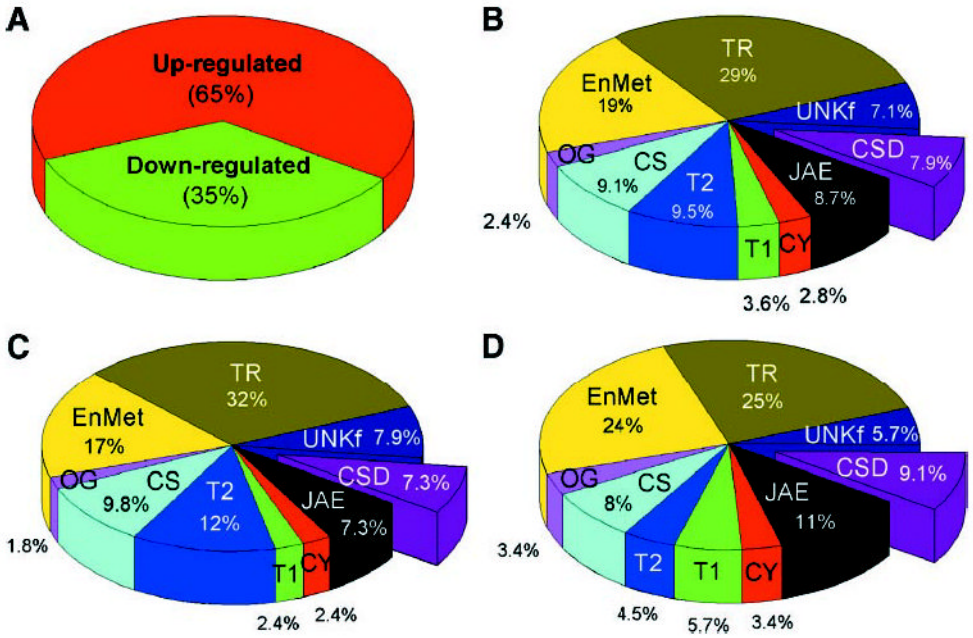

Fig. 2.

Categorization of significantly ($P < 0.05$) altered expression of identified genes in Cx43-null compared with WT astrocytes. *A*: of the 252 significantly altered identified genes, 35% (88 genes) were downregulated and 65% (164) were upregulated. *B*: distribution of altered genes in functional categories. JAE, junction-adhesion-extracellular matrix; CY, cytoskeletal; T1, transport into the cell; T2, transport within the cell; CS, cell signaling; CSD, cell cycle-shape-differentiation; TR, transcription; EnMet, energy and metabolism; OG, organelle genetics; UNKf, unknown function. See text for expanded description of categories. *C* and *D*: relative percentages of up- and downregulated genes of each functional category in astrocytes of Cx43-null compared with WT mice.

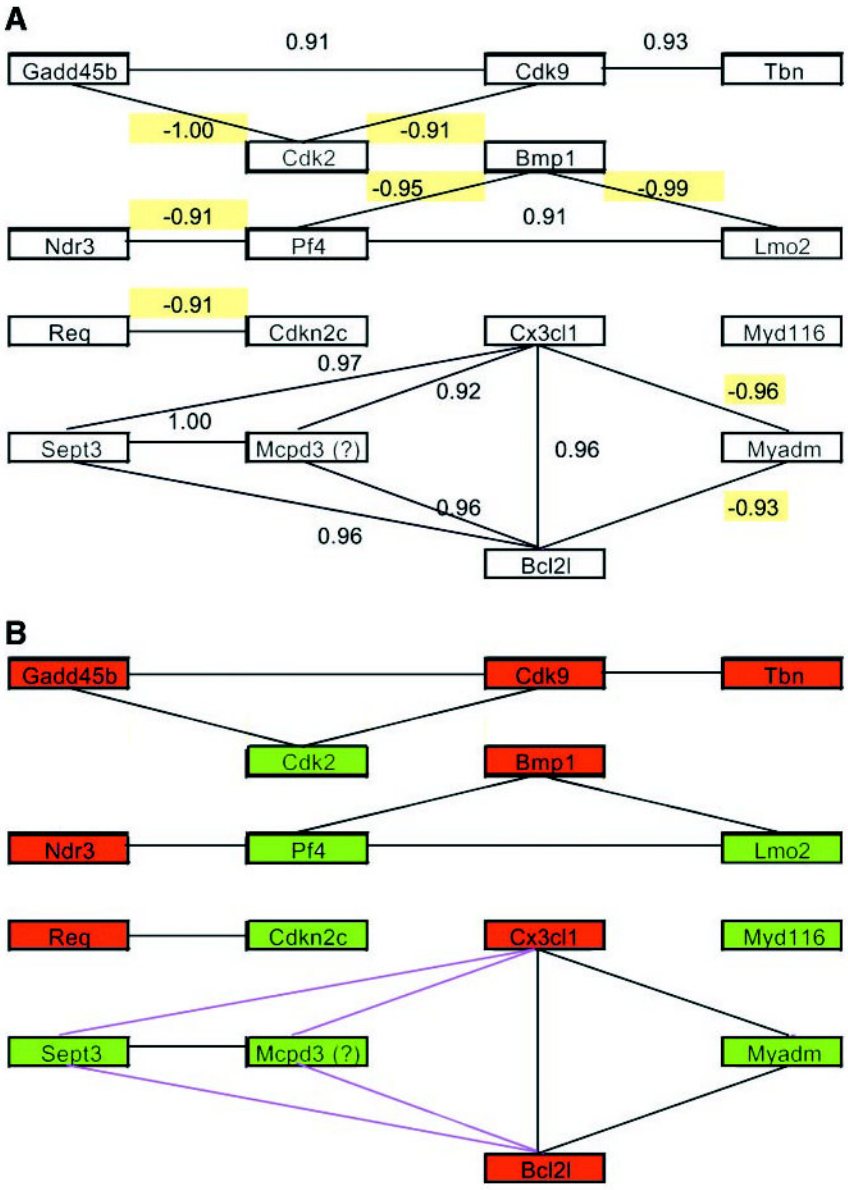

Fig. 3.

Significant ($P < 0.05$) coordination among the expression of cell cycle-shape-differentiation (CSD) genes in WT cortical astrocytes (*A*) that were significantly regulated in the Cx43-null astrocytes (*B*). Gene designations are within boxes; lines between boxes indicate significant coordinations of the expression of paired genes in the WT cortical astrocytes (numbers atop lines provide correlation coefficients; antagonistic coordinations are highlighted in yellow). Colors of boxes in *B* indicate whether a gene was significantly upregulated (red) or downregulated (green) in Cx43-null astrocytes. Red lines in the cluster at the *bottom* indicate that regulation in Cx43 KO samples was opposite to that predicted by the coordination analysis in the WT astrocytes.

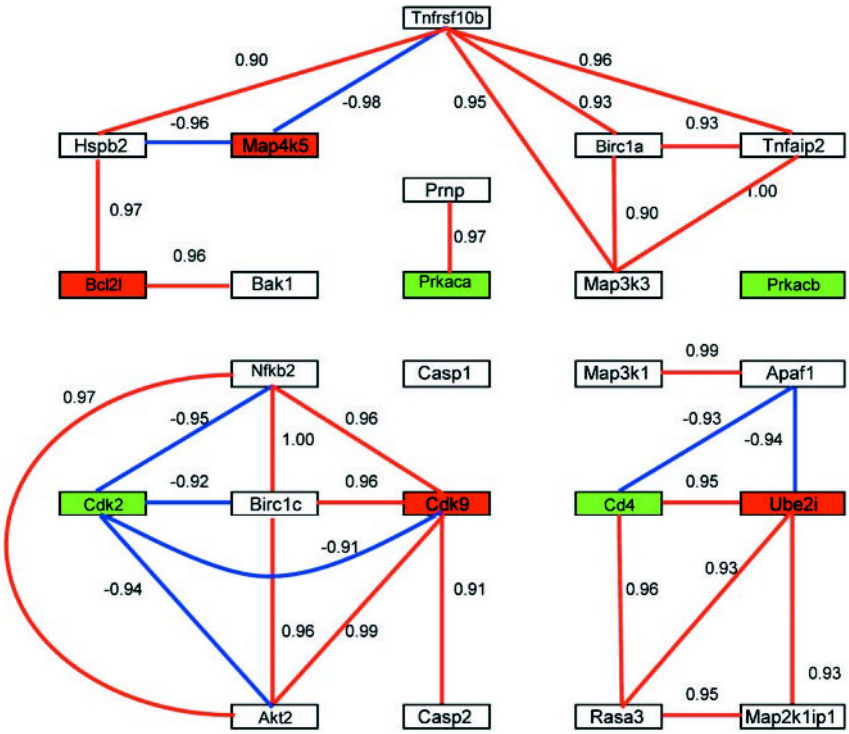

Fig. 4.

Significant coordinations among the expression of genes related to programmed cell death in WT cortical astrocytes. Gene designations are within boxes; lines between boxes indicate significant coordinations of the expressions of paired genes in the WT cortical astrocytes (values on lines provide correlation coefficients). Colors of boxes indicate whether a gene was significantly upregulated (red) or downregulated (green) in Cx43-null astrocytes, while colors of lines indicate whether the coordination was synergistic (blue) or antagonistic (red).

Table 1

Experimental design

Step	Hybridization	Purpose
α	RrRg RrRg	"Yellow test" to check the printing quality, verify the hybridization efficiency, test the relevancy of gene expression within the reference, and determine the PMT settings
β	RrWT(*1*)g RrWT(*2*)g RrWT(*3*)g RrWT(*4*)g	Estimate the expression variability and stability in WT cortical astrocytes
γ	RrKO(*1*)g RrKO(*2*)g RrKO(*3*)g RrKO(*4*)g	Estimate expression variability and stability in Cx43-null cortical astrocytes and determine expression ratios and scores

cDNA array spot intensities were analyzed in three steps (α, β, γ), using the number of arrays and type of hybridization indicated. In the α-step, two arrays were hybridized with reference (*R*) cDNA, half of which was labeled with the red fluorophore Cy5 (r) and half with green Cy3 (g), to correct for differences in photomultiplier voltages (PMT settings). In the β-step, RNA extracted from cultured wild-type (WT) astrocytes from four animals (indicated as *1*. . . *4*) was labeled with green fluorophore and hybridized against red labeled reference (Rr) to establish the variability of hybridization to each spotted sequence among the WT astrocytes. In the γ-step, green-labeled cDNA from four connexin-43 (Cx43)-null mice (KO, indicated *1*. . .*4*) was hybridized against the red-labeled reference to measure variance. Finally, expression ratios (*x*) were determined for each spot, and expression scores (τ) were calculated based on the hybridization variances, to test the statistical significance of the observed regulations.

Table 2

The least variably (i.e., most stably) expressed genes in WT neonatal mouse cortical astrocytes and corresponding values in Cx43-null astrocytes

Notes	GenBank ID	Description	REV-WT	GES-WT	REV-KO	GES-KO
	AA032414	synaptosomal-associated protein, 25 kDa, binding protein	4.93	99.84	59.61	33.04
1	AA068478	ganglioside-induced differentiation-associated protein 2	5.78	99.80	14.29	95.99
	AA471915	cytochrome *P*-450, 21, steroid 21 hydroxylase	5.81	99.77	60.06	32.40
	AA185691	solute carrier family 12, member 4	5.89	99.74	35.83	66.94
	AA170564	Son cell proliferation protein	6.51	99.60	29.35	76.98
	AA221269	cleavage and polyadenylation specific factor 2, 100kDa subunit	6.63	99.57	37.99	63.99
	AA033370	Williams-Beuren syndrome chromosome region 1 homolog (human)	7.03	99.51	21.69	88.28
A	W14960	immunoglobulin kappa chain, joining region	7.11	99.47	123.14	4.87
	W42224	synaptotagmin 4	7.23	99.41	64.04	28.78
	AA003173	monocyte macrophage 19	7.60	99.27	25.78	82.77
B	AA008503	procollagen-lysine, 2-oxoglutarate 5-dioxygenase 1	7.75	99.21	134.64	3.67
	W62969	Fyn proto-oncogene	8.01	99.11	19.54	91.01
	AA544321	Sjogren syndrome antigen B	8.37	99.04	57.61	35.21
	AA098608	proteasome (prosome, macropain) subunit, alpha type 7	8.42	99.01	12.95	29.03
	AA050453	purinergic receptor P2X, ligand-gated ion channel 4	8.54	98.98	63.73	40.08
	AA198703	apoptotic protease activating factor 1	8.76	98.85	85.40	40.80
	AA272198	uroporphyrinogen III synthase	8.78	98.81	52.90	79.40
	AA458128	putative RNA helicase	9.22	98.71	27.86	93.63
	AA399854	asparaginyl-tRNA synthetase	9.47	98.68	17.06	35.46
	AA538330	paralemmin	9.62	98.65	57.41	16.81
	AA517145	L-threonine dehydrogenase	9.83	98.58	79.08	11.33
	AA034847	peroxisomal protein (PeP)	10.01	98.52	92.25	9.77
2	AA212963	Zinc finger protein 275	10.75	98.19	21.14	99.44
	AA000219	eukaryotic translation initiation factor 2B	10.96	98.12	6.67	71.14
	AA051096	nuclear receptor-binding SET-domain protein 1	11.04	98.09	33.15	75.65
	AA277830	angiopoietin-like 3	11.06	98.05	30.14	29.95
	AA231621	glutathione transferase zeta 1 (maleylacetoacetate isomerase)	11.38	97.99	62.88	53.02

Notes	GenBank ID	Description	REV-WT	GES-WT	REV-KO	GES-KO
	AA241780	ATPase, H^+ transporting, lysosomal interacting protein 1	11.54	97.92	44.76	48.12
	AA403531	E2F transcription factor 6	11.57	97.86	47.86	73.89
	AA289983	CD2 antigen (cytoplasmic tail) binding protein 2	11.66	97.82	31.50	25.02
	AA387258	myosin IB	11.68	97.76	68.40	66.85
	AA512478	cytochrome *c* oxidase, subunit VIIa 3	11.81	97.69	35.86	70.41
	AA161846	ras association (RaIGDS/AF-6) domain family 1	11.92	97.63	33.56	64.63
	AA245451	mitochondrial ribosomal protein S16	12.03	97.59	37.32	91.82
3	AA277958	proteasome (prosome, macropain) subunit, alpha type 4	12.17	97.56	18.76	98.22
	AA031130	RNA polymerase II 3	12.19	97.46	10.05	11.05
	AA275684	bile acid-coenzyme A: amino acid *N*-acyltransferase	12.21	97.43	93.49	89.54
	W67089	early development regulator 2 (homolog of polyhomeotic 2)	12.25	97.39	20.97	58.78
	W41459	eukaryotic translation initiation factor 1A	12.52	97.30	41.27	40.44
	AA003924	protein kinase C substrate 80K-H	12.54	97.16	53.11	70.67
	AA217687	adaptor-related protein complex AP-3, sigma 1 subunit	12.88	96.93	80.95	40.52
	AA276030	ATPase, H^+ transporting, lysosomal 16 kDa; V0 subunit c	12.91	96.87	53.07	62.29
	AA017848	cytokine inducible SH2-containing protein 3	12.95	96.83	39.04	49.85
	AA111040	kinesin family member 5B	13.13	96.77	46.76	25.58
	AA498185	makorin, ring finger protein, 2	13.23	96.67	67.78	15.53
	AA230925	inositol 1, 4, 5-triphosphate receptor 1	13.31	96.54	80.81	68.44
	W91307	peroxiredoxin 3	13.43	96.47	34.94	87.59
4	AA271411	ubiquitin conjugating enzyme 7 interacting protein 3	13.51	96.37	22.24	97.66
	AA237820	melanoma antigen, family D, 3	13.52	96.34	11.54	68.02
	W08703	WD40 protein Ciao1	13.73	96.17	35.26	63.87
	AA108948	tripartite motif protein 8	13.80	96.14	38.09	31.70
	AA138529	zinc finger protein 62	13.82	96.11	60.75	84.50
5	W34482	torsin family 3, member A	13.88	96.08	24.51	97.02
	W08452	X-ray repair complementing defective repair in Chinese hamster cells 1	14.11	95.84	12.70	62.43
6	AA061868	adaptor-related protein complex AP-1, mu subunit 1	14.13	95.81	38.95	96.02
	W11186	mitochondrial ribosomal protein L19	14.18	95.75	14.26	44.92
	AA073211	ubiquitin-like 1 (sentrin) activating enzyme E1A	14.21	95.68	50.09	43.08

Notes	GenBank ID	Description	REV-WT	GES-WT	REV-KO	GES-KO
	W64529	high mobility group 20A	14.27	95.65	51.15	26.33
	AA511176	zinc finger protein 207	14.34	95.58	67.08	20.15
	AA268608	squalene epoxidase	14.88	95.25	86.43	26.52

REV, relative estimated variability; GES, gene expression stability; KO, knockout. Notes are addressed in text.

Table 3

The most variably expressed genes in WT astrocytes and corresponding values in Cx43-null astrocytes

Notes	GenBank ID	Description	REV-WT	GES-WT	REV-KO	GES-KO
	AA538426	translocated promoter region protein	317.10	0.03	121.74	4.98
	AA387076	A kinase (PRKA) anchor protein (gravin) 12	193.29	0.20	109.38	6.76
	AA109041	calmodulin 3	185.07	0.26	60.40	32.09
	W97837	protein kinase, DNA activated, catalytic polypeptide	172.19	0.33	67.00	26.41
1	AA064011	aquaporin 1	158.26	0.46	291.54	0.45
2a	**AA000678**	**biglycan**	**150.07**	**0.69**	**228.78**	**1.03**
	AA172527	ATP-binding cassette, sub-family G (WHITE), member 1	147.68	0.73	189.56	1.81
	AA145458	fibronectin 1	143.88	0.79	199.98	1.42
	W89883	procollagen, type III, alpha 1	141.08	0.86	376.91	0.06
	W83904	peptidylprolyl isomerase C	140.99	0.89	222.57	1.11
	W99037	proteasome (prosome, macropain) 26S subunit, non-ATPase, 5	139.95	0.92	90.25	11.75
	W80177	type IV collagenase	139.61	0.96	227.98	1.09
	AA098099	cadherin 11	136.20	1.06	75.62	18.93
	AA388435	peroxisomal sarcosine oxidase	134.85	1.09	131.51	4.04
2b	**AA200264**	**biglycan**	**130.61**	**1.19**	**230.82**	**1.00**
3	AA059909	secreted modular calcium binding protein 2	124.61	1.42	368.60	0.11
	AA050726	paired related homeobox 1	123.97	1.45	63.57	29.22
	W76877	thioredoxin interacting protein	121.48	1.48	99.28	9.32
	W11644	translocator of inner mitochondrial membrane 17 kDa, a	119.64	1.58	37.73	64.24
	AA172598	ATPase, Na+/K+ transporting, alpha 4 polypeptide	118.45	1.68	37.47	64.46
	AA051330	SWI/SNF related, matrix associated, actin dependent chromatin regulator	117.83	1.72	50.77	43.72
	AA027478	G protein-coupled receptor kinase-interactor 2	113.22	1.88	194.22	1.67
	AA028539	platelet-derived growth factor, C polypeptide	110.98	2.01	65.99	27.22
	W33786	procollagen, type VI, alpha 1	110.16	2.08	214.09	1.25
2c	**W54287**	**biglycan**	**108.69**	**2.18**	**271.21**	**0.56**
	W18828	dihydropyrimidinase-like 3	108.48	2.21	121.79	4.95
	AA023221	inositol hexaphosphate kinase 1	108.23	2.24	80.71	15.56
	AA061732	shroom	107.97	2.28	105.15	7.82
	AA139817	nuclear fragile X mental retardation protein interacting protein	107.77	2.31	76.81	18.12

Notes	GenBank ID	Description	REV-WT	GES-WT	REV-KO	GES-KO
	AA110412	myeloid differentiation primary response gene 88	106.83	2.41	84.76	13.61
	W08937	neutral sphingomyelinase (N-SMase) activation associated factor	106.57	2.47	55.81	37.24
	AA177363	ectonucleotide pyrophosphatase/phosphodiesterase 2	106.11	2.51	94.61	10.69
	AA119255	ribosomal protein L13a	106.08	2.54	46.82	49.71
	AA060697	zinc finger protein 261	106.02	2.57	76.29	18.45
	AA116505	CD53 antigen	105.00	2.67	199.16	1.45
	AA176035	polycystic kidney disease 2	104.42	2.70	26.53	81.58
	AA060905	guanosine diphosphate (GDP) dissociation inhibitor 1	104.38	2.74	64.28	28.56
	AA051390	protein (peptidyl-prolyl cis/trans isomerase) NIMA-interacting 1	104.14	2.77	32.24	72.56
4	AA475004	low density lipoprotein receptor	100.59	2.90	304.01	0.25
	AA105153	neurofibromatosis 2; schwannomin; moesin-ezrin-radixin-like protein	100.09	2.94	40.99	59.23
	AA220047	zinc finger protein 60	99.80	2.97	35.72	67.21
	AA543167	coilin	99.48	3.00	29.01	77.57
	AA509751	fused toes	99.36	3.03	112.15	6.26
	AA239404	nidogen 1	99.33	3.07	99.28	9.35
	AA032394	sarcoma viral (v-yes-1) oncogene homolog	99.17	3.10	127.81	4.29
	AA097314	abhydrolase domain containing 3	98.53	3.20	100.12	9.05
	W34612	transglutaminase 2, C polypeptide	98.52	3.23	72.81	21.43
	AA273927	DEAD (aspartate-glutamate-alanine-aspartate) box polypeptide, Y Chr	98.16	3.27	108.46	7.07
A	AA067191	UDP-glucose dehydrogenase	97.84	3.43	17.30	93.49
	AA521755	solute carrier family 7 (cationic amino acid transporter, y + system)	97.65	3.50	110.86	6.48
B	AA538508	ribosomal protein L44	97.28	3.53	17.77	92.90
	AA423717	AP endonuclease 2	97.14	3.56	33.60	70.36
	AA003272	heat shock protein 20-like protein	96.70	3.59	99.35	9.30
	W09867	small nuclear ribonucleoprotein polypeptide F	94.54	4.02	90.94	11.66
	W91228	putative phosphatase	94.44	4.09	65.21	27.86
	W82406	laminin, gamma 1	92.96	4.42	68.16	25.19
	AA033292	bone morphogenetic protein 1	91.82	4.65	98.83	9.52
	AA038087	DiGeorge syndrome critical region gene 2	90.16	4.98	80.84	15.47
	AA144286	hemopoietic cell phosphatase	89.67	5.11	193.25	1.73

Notes	GenBank ID	Description	REV-WT	GES-WT	REV-KO	GES-KO
	AA242315	TYRO protein tyrosine kinase binding protein	89.56	5.15	99.54	9.18

REV and GES are defined in Table 2. Note the similarity of the values obtained for the three distinct spotted sequences homologous to biglycan: AA000678 [HS = 407, $p(N) = 1.1 \times 10^{-11}$], AA200264 [HS = 2014, $p(N) = 1.1 \times 10^{-85}$], W54287 [HS = 2970, $p(N) = 7.2 \times 10^{-129}$], which reinforces confidence in the accuracy of our transcription stability analysis. Notes are discussed in the text.

Table 4

The coordination power (COP), gene expression stability (GES) and gene prominence (GP) of the significantly regulated CSD genes in Cx43 KO astrocytes

GenBank ID	Gene Description	Symbol	COP	GES	GP	$\log_2 x$	*P* Value
W64388	growth arrest and DNA-damage-inducible 45 beta	Gadd45b ↑	6.81	88.26	11.81	0.76	0.034
AA124465	cyclin-dependent kinase 2	Cdk2 ↓	6.73	87.93	11.62	−0.50	0.002
W85480	cyclin-dependent kinase 9 (CDC2-related kinase)	Cdk9 ↑	6.08	84.07	10.04	0.28	0.015
AA000862	taube nuss	Tbn ↑	5.65	83.48	9.27	0.22	0.050
AA185249	Similar to mitotic control protein dis3	Mcpd3? ↓	6.75	80.38	10.66	−3.91	0.006
AA423252	cyclin-dependent kinase inhibitor 2C (p18, inhibits CDK4)	Cdkn2c ↓	4.91	66.33	6.40	−0.49	0.027
AA051441	Bcl2-like	Bcl2l ↑	6.76	56.04	7.45	0.53	0.011
AA272232	chemokine (C-X3-C motif) ligand 1 (fractalkine)	Cx3cl1 ↑	6.32	50.79	6.31	0.88	0.017
AA231566	myeloid-associated differentiation marker	Myadm ↓	6.41	46.64	5.88	−0.42	0.041
AA014819	platelet factor 4	Pf4 ↓	6.50	44.00	5.62	−0.99	0.012
AA118721	requiem	Req ↑	5.43	35.52	3.79	0.51	0.029
AA290294	LIM only 2	Lmo2 ↓	6.34	26.45	3.30	−0.54	0.047
AA050417	myeloid differentiation primary response gene 116	Myd116 ↑	6.24	18.11	2.22	0.59	0.043
W82677	bone morphogenetic protein 1	Bmp1 ↑	6.49	16.29	2.08	0.74	0.008
AI605734	septin 3	Sept3 ↓	6.63	15.93	2.08	−0.76	0.048
AA213094	N-myc downstream regulated 3	Ndr3 ↑	5.95	12.63	1.48	0.69	0.044

Up arrows indicate upregulated genes; down arrows indicate downregulated genes. Column labeled “log” provides the $\log_2$ of the expression ratio, and *P* value indicates level of significance.